Design of L-band Energy-Selective Surface with Circular Ring Gap

Guohui Yang [1], Yong Li [1], Qun Wu [1], Yan Wang [2], and Yingsong Li [3,*]

[1] School of Electronic and Information Engineering, Harbin Institute of Technology, Harbin 150001, China

[2] Shenyang Aircraft Design and Research Institute, AVIC, Shenyang 110000, China

[3] College of Information and Communication Engineering, Harbin Engineering University, Harbin 150001, China
gh.yang@hit.edu.cn, liyingsong@ieee.org*

Abstract ─ An narrow-band energy-selective surface (ESS) in L-band is presented for airborne GPS antenna protection. Periodic square metal inlaid with circular ring gap is designed and loaded with pin diodes to obtain the energy selection characteristics. the parameters of unit structure are determined with optimization. By simulation, we know that the insertion loss is less than 3dB and the shielding efficiency is more than 30dB. Using the method of equivalent test, we experimentation verified that the proposed ESS structure can be used for airborne GPS antenna protection

Index Terms ─ Circular ring gap, energy selective surface, pin diodes, self-actuated protection.

I. INTRODUCTION

Around 1960, EMP began to receive the attention of the military. EMP weapons have been developing rapidly [1]. At the same time, the electromagnetic protection structure based on frequency selective surface has been developed, such as hybrid radome, band stop filter, etc. [2]. FSS is widely used, such as antenna array decoupling and beamforming [3-6]. However, although FSS can effectively reduce the electromagnetic pulse outside the passband, it can't protect the pulse inside the passband. This led to the emergence of ESS. ESS is a kind of self-adaptive protection structure which using the structure of FSS controlled by the electric field sensitive device, it can pass the low-power signal and shield the high-power signal in the same frequency band.

At present, using diode as the energy selective surface design of electronic control device is the mainstream practice. Corresponding to the on state and off state of diode under the excitation of induced voltage, ESS also have two states of high-power state and small signal state. As the name suggests, high power state is to use the band stop characteristic of FSS to protect the strong electromagnetic pulse, and small signal state is to use the band-pass characteristic of FSS to ensure that the small signal can pass normally. In fact, ESS is FSS which can adaptively switch the above two states. When ESS is irradiated by the high power electromagnetic pulse, the electronic characteristic structure of ESS will be changed from the band-pass structure (small signal state) to the band stop structure (high power state) in the most ideal situation. There are two main design ideas in ESS using diode. One design idea is based on band stop frequency selection surface. When ESS is in small signal state, resonance frequency should be far away from working frequency band to ensure normal passing of small signal. When ESS is in high power state, resonance frequency should be consistent with working frequency band to shield large signal pulse. The cross strip structure designed by this design idea has been proved to have good performance in [7]. However, this design idea also has disadvantage, in order to keep the resonant frequency as far away from the working frequency band as possible, it is necessary to make the unit very small, which will make the diode number of the whole ESS become a lot, resulting in processing difficulties and high costs. Another design idea can effectively avoid this problem that is based on a band pass frequency selection surface. When ESS is in small signal state, resonance frequency should work in working frequency band to ensure normal passing of small signal. When ESS is in high power state, resonance frequency should far away from working frequency band to shield large signal pulse. Because the working frequency of the antenna is in the L-band, the size of the unit is generally large, and the diodes used in each unit will not increase too much, so the diodes used in the whole ESS are greatly reduced. The structure proposed in this paper is designed according to the second design idea, and its advantages of low cost and easy processing will be seen below.

In this paper, an ESS in L-band is designed and optimized. Electromagnetic simulations are carried out by CST Microwave Studio and the results show that the

Submitted On: February 25, 2020
Accepted On: April 20, 2020

presented ESS structure has good performance in 1.5-1.57GHz. The proposed structure has small size and simple structure, which is easy to applicated.

II. ESS UNIT AND ANALYSIS

A. Structure introduction

The unit of ESS designed in this paper is shown in Fig. 1 and Fig. 2. It consists of a square metal surface inlaid with a circular ring gap. The ring gap structure has band-pass characteristics. The resonance frequency is determined by choosing the appropriate unit size. Connect 4 diodes across the gap. In this way, when it is not enough to trigger the small signal of diode conduction to pass through, it can be ensured to pass normally by the same characteristics. When a large signal is incident, the diode turns on and the ESS switches to the high power state.

As is shown in Fig. 1 and Fig. 2, the parameters are side length equals to 46.6 mm, r = 21 mm, patch = 46.4 mm, h = 0.7 mm and gap = 1.5 mm. The dielectric board material is FR4, the dielectric constant is 4.3, the patch metal is pure copper. Based on the principle of small transmission coefficient in forward bias and large transmission coefficient in reverse bias, by comparing the S parameter of diodes, we finally choose BAP70-03.

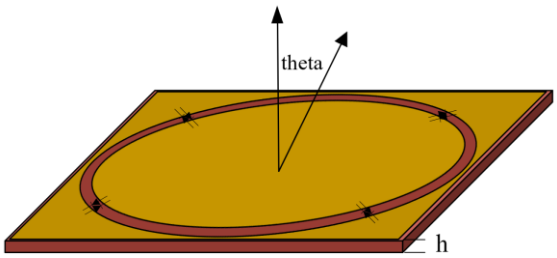

Fig. 1. Structure of ESS unit.

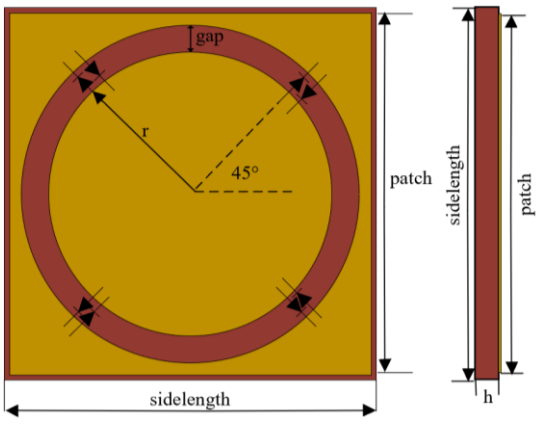

Fig. 2. ESS unit front view and side view.

B. Simulation results of CST software

For the convenience of simulating diode in CST, we choose the diode equivalent model in [8-12] which is shown in Fig. 3, where the boundary is unit cell.

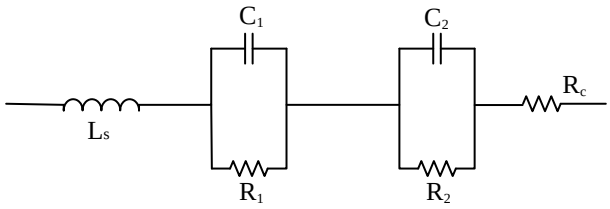

Fig. 3. Diode equivalent circuit.

And then, the S-parameter data of the selected diode is imported into ADS, confirming that it is consistent with the datasheet. Then, we establish the diode equivalent circuit model. By using the optimization function of ADS software, the equivalent circuit of the diode in the reverse and forward biases is obtained in Fig. 4 and Fig. 5.

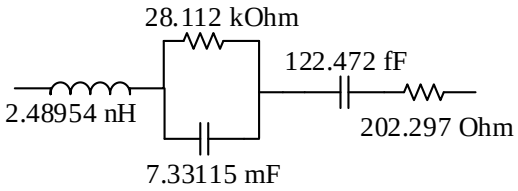

Fig. 4. Disconnected state equivalent circuit.

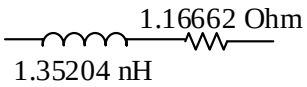

Fig. 5. Conduction state equivalent circuit.

Take the equivalent model into CST, and get the Transmission coefficient and shielding effectiveness curve as shown in the Fig. 6. In the simulation, we found that the number of the diodes will affect the performance of the ESS. If many diodes are used in the ESS, the transmission performance will get worse, while the shielding behaviour will get better, and vice versa. Thus, we give an example in Fig. 2 to discuss the design of the ESS.

The incident angle has an effect on the bandwidth, resonance frequency, transmission performance, shielding performance and other indicators of ESS. In practical application, the incident direction cannot always be vertical, so to study the stability of ESS performance at large angle of incidence, the incident angle was set from 0° to 45°.The results are shown in Fig. 7 and Fig. 8.

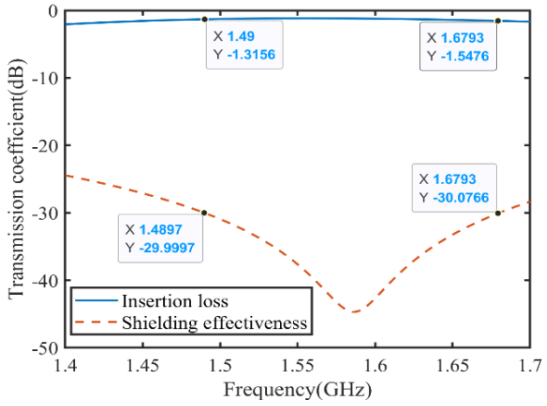

Fig. 6. Insertion loss and shielding effectiveness at normal incidence.

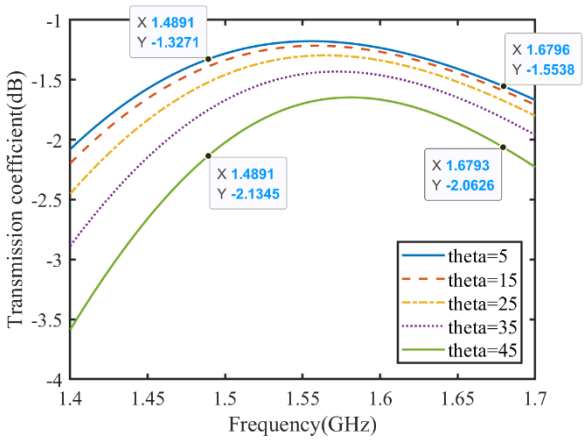

Fig. 7. Transmission coefficient varies with the incident angle.

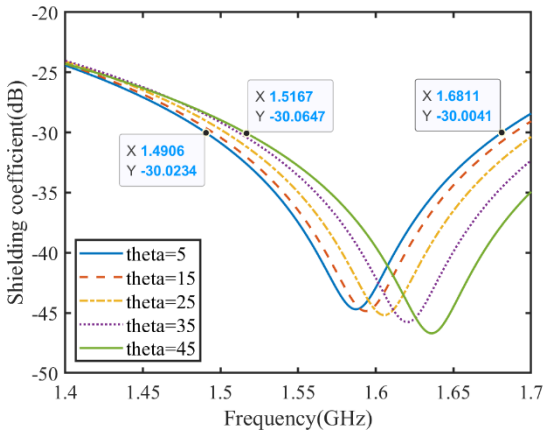

Fig. 8. Shielding effectiveness varies with the incident angle.

As shown in Fig. 6, it can be seen that the bandwidth of 30 dB shielding coefficient is about 210 MHz. the insertion loss is less than 2dB. From Fig. 7 and Fig. 8, with the increase of incident angle, the insertion loss and shielding coefficient increase slightly, but the consistency is wonderful. So far, after simulation and optimization, we have determined that the size of the cell is 46.6mm ≈ 0.215λ, and each cell uses four diodes. The design of ESS has been completed.

III. EXPERIMENTAL VALIDATION

A. Fabrication and experiment

To verify the performance of ESS, a prototype including 7×7 cells is fabricated as shown in Fig. 9, and a 15mm space is reserved around the patch to fix the printed circuit.

B. Test Result

According to the shielding effectiveness measurement method of electromagnetic shielding materials mentioned in military standard GJB6190-2008, build the test block diagram as shown in Fig. 10 and the test environment as shown in Fig. 11 and Fig. 12.

Because it is very difficult to produce EMP, the proposed test method is to use two test boards that have been processed, manually change their working conditions, and then use the low-power incident wave for testing. The diode on one test board does not do any processing, which is considered to work in the wave transmission state. The other uses solder instead of diode to simulate the shielding state. The test results are as shown in Fig. 13.

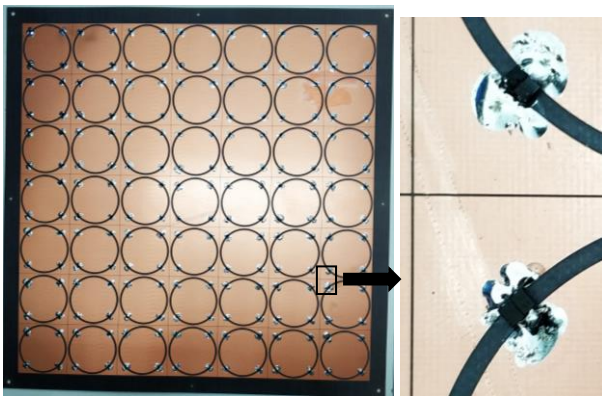

Fig. 9. Photograph of the ESS prototype

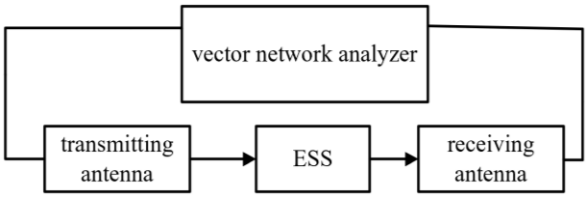

Fig. 10. Test diagram.

Fig. 11. Test environment (front side).

Fig. 12. Test environment (back side).

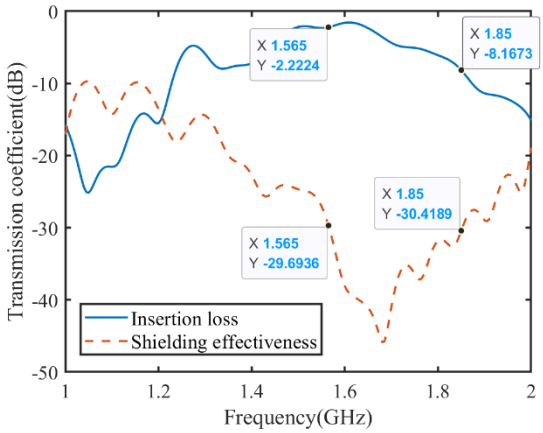

Fig. 13. Insertion loss and shielding effectiveness at normal incidence.

From Fig. 13, it can be seen that the shielding curve reaches 29.69 dB at 1.565 GHz. At this time, the insertion loss is about 2.2 dB, which generally meets the design requirements. Comparing the simulation Fig 6 with the test result Fig. 13, it can be found that the center frequency of the shielding effectiveness stopband is shifted about 200 MHz to the high frequency direction. This is because the diode will have an impact on the resonant frequency point. Replacing the diode with solder will cause the resonant frequency point to move.

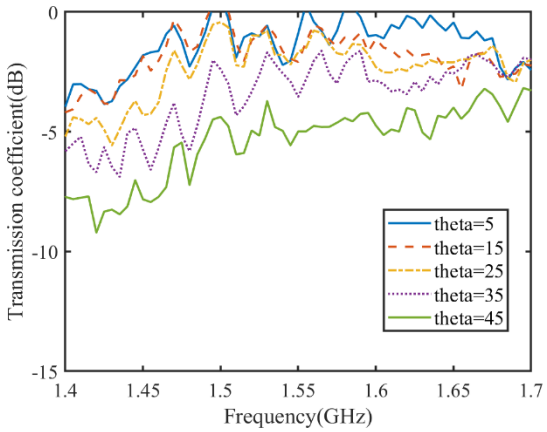

Fig. 14. Transmission coefficient varies with the incident angle.

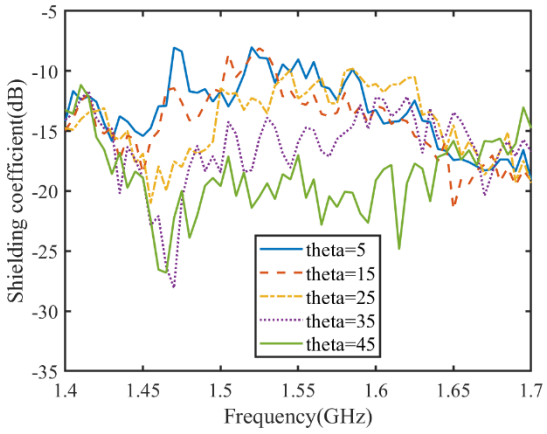

Fig. 15. Shielding effectiveness varies with the incident angle.

Next, verify the stability of ESS at large angle of incidence, and the test results are shown in Fig. 14 and Fig. 15. From the test results, it can be seen that at the working frequency of 1.565 GHz of the Airborne GPS antenna, the insertion loss slightly increases with the incident angle increasing, but it still does not exceed 3 dB, and the shielding efficiency is not less than 30 dB, which is in line with the expected effect, which proves that the designed unit structure has practical value and theoretical guidance significance.

IV. CONCLUSION

A narrow-band ESS in L-band is presented in this paper. The proposed ESS has an operating frequency at 1.565 GHz and operating band from 1.49 GHz to 1.68 GHz. Diode equivalent circuit model was used for simulation. On this basis, we verify the stability of large angle incident. Both simulation and experiments result show that the insertion loss of the structure is less than 3 dB at 1.565 GHz, and the shielding efficiency is more than 30 dB, which meets the design requirements. It can be used for high power microwave protection of Airborne GPS antenna. In the future, we will consider the application for circular polarization antennas [13] and use the adaptive method to control the diodes [14-15] for array applications [16].

ACKNOWLEDGMENT

This work was supported in the Fundamental Research Funds for the Central Universities (3072020CFT0802) and the Key Research and Development Program of Heilongjiang (GX17A016) and Open Project of State Key Laboratory of Millimeter Waves (K202017).

REFERENCES

[1] C. E. Baum, "Reminiscences of high-power electromagnetics," *IEEE Transactions on Electromagnetic Compatibility*, vol. 49, no. 2, pp. 211-218, 2007.

[2] B. A. Munk, *Frequency Selective Surface, Theory and Deisgn*. Wiley, 2000.

[3] F. Liu, J. Guo, L. Zhao, G. Huang, Y. Li, and Y. Yin, "Dual-band metasurface-based decoupling method for two closely packed dual-band antennas," *IEEE Transactions on Antennas and Propagation*, vol. 68, no. 1, pp. 552-557, Jan. 2020.

[4] K. Yu, Y. Li, and X. Liu, "Mutual coupling reduction of a MIMO antenna array using 3-D novel meta-material structures," *Appl. Comput. Electromagn. Soc. J*., vol. 33, no. 7, pp. 758-763, 2018.

[5] J. Jiang, Y. Xia, and Y. Li, "High isolated X-band MIMO array using novel wheel-like metamaterial decoupling structure," *Appl. Comput. Electromagn. Soc. J*., vol. 34, no. 12, pp. 1829-1836, 2019.

[6] S. Luo, Y. Li, Y. Xia, et al., "Mutual coupling reduction of a dual-band antenna array using dual-frequency metamaterial structure," *Applied Computational Electromagnetics Society Journal*, vol. 34, no. 3, pp. 403-410, 2019.

[7] C. Yang, P. Liu, and X. Huang, "A novel method of energy selective surface for adaptive HPM/ EMP protection," *IEEE Antennas and Wireless Propagation Letters*, vol. 12, pp. 112-115, 2013.

[8] R. F. Harrington, *Time-Harmonic Electromagnetic Fields*. McGraw-Hill, New York, 1961.

[9] S. Shin and S. Kanamaluru, "Diplexer design using EM and circuit simulation techniques," *IEEE Microwave Magazine*, vol. 8, no. 2, pp. 77-82, Apr. 2007.

[10] V. Rizzoli, A. Costanzo, D. Masotti, and P. Spadoni, "Circuit-level nonlinear electromagnetic co-simulation of an entire microwave link," *IEEE MTT-S Int. Microwave Symp. Dig*., Long Beach, CA, pp. 813-816, June 2005.

[11] Ansoft High Frequency Structure Simulation (HFSS), ver. 10, Ansoft Corporation, Pittsburgh, PA, 2005.

[12] W. Rufei, Z. Haiying, Y. Junjian, et al., "A novel equivalent circuit model of GaAs PIN diodes," *Journal of Semiconductors*, vol. 29, no. 4, pp. 672-676, 2008.

[13] K. L. Chuang, X. Yan, Y. Li, and Y. Li, "A Jia-shaped artistic patch antenna for dual-band circular polarization," *AEÜ- International Journal of Electronics and Communications*, 10.1016/ j.aeue.2020.153207.

[14] Y. Li, Z. Jiang, O. M. Omer-Osman, et al., "Mixed norm constrained sparse APA algorithm for satellite and network echo channel estimation," *IEEE Access*, vol. 6, pp. 65901-65908, 2018.

[15] Y. Li, Y. Wang, and T. Jiang, "Sparse-aware set-membership NLMS algorithms and their application for sparse channel estimation and echo cancelation," *AEU - International Journal of Electronics and Communications*, vol. 70, no. 7, pp. 895-902, 2016.

[16] X. Zhang, T. Jiang, and Y. Li, "A novel block sparse reconstruction method for DOA estimation with unknown mutual coupling," *IEEE Communications Letters*, vol. 23, no. 10, pp. 1845-1848, 2019.